Saudi Pharmaceutical Journal 32 (2024) 101999

HOSTED BY

Contents lists available at ScienceDirect

Saudi Pharmaceutical Journal

journal homepage: www.sciencedirect.com

# Development of nanoemulgel of 5-Fluorouracil for skin melanoma using glycyrrhizin as a penetration enhancer

Nimish Gupta [a], G.D. Gupta [a], Karan Razdan [b], Norah A. Albekairi [c], Abdulrahman Alshammari [c], Dilpreet Singh [a,d,*]

[a] Department of Pharmaceutics, ISF College of Pharmacy, GT Road, Moga 142001, Punjab, India
[b] University Institute of Pharmaceutical Sciences, Panjab University, Chandigarh, India
[c] Department of Pharmacology and Toxicology, College of Pharmacy, King Saud University, Riyadh 11451, Saudi Arabia
[d] University Institute of Pharma Sciences, Chandigarh University, Gharuan (140413), Mohali, India

ARTICLE INFO

*Keywords:*
5-FU
Nanoemulsion
Nanoemulsion based gel
Cytotoxicity
Permeation
Solubility
Melanoma
Targeting

ABSTRACT

The purpose of this study was to enhance the topical delivery of 5-Fluorouracil (5-FU), a cancer treatment, by developing a nanoemulgel formulation. Glycyrrhizin (GLY), a natural penetration enhancer has been investigated to exhibit synergistic effects with 5-FU in inhibiting melanoma cell proliferation and inducing apoptosis, Hence, GLY, along with suitable lipids was utilized to create an optimized nanoemulsion (NE) based gel. Solubility studies and ternary phase diagram revealed isopropyl myristate (IPM), Span 80, Tween 80 as $S_{mix}$ and Transcutol P as co-surfactant. IPM demonstrates excellent solubilizing properties facilitates higher drug loading, ensuring efficient delivery to the target site.,The optimized formulation consisting of 40 % IPM, 30 % of mixture of Tween80: Span80 ($S_{mix}$) and 15 % Transcutol P provides with a nanometric size of 64.1 ± 5.13 nm and drug loading of 97.3 ± 5.83 %. The optimized formulation observed with no creaming and breakeing of NE and found thermodynamically stable during different stress conditions (temperatures of 4.0 °C and 45.0 °C) and physical thawing (−21.0 ± 0.50 °C to 20.0 ± 0.50 °C). The NE was then transformed into a nanoemulgel (NEG) using 1.5 % w/w Carbopol base and 0.1 % *w/w* glycyrrhizin. The *ex vivo* permeability studies showed significant enhancements in drug permeability with the GLY-based 5-FU-NEG formulation compared to pure 5-FU gel in excised pig skin upto1440 min in PBS 7.4 as receptor media. The $IC_{50}$ values for Plain 5-FU gel, 5-FU-NEG, and GLY-based 5-FU-NEG were found to be 20 μg/mL, 1.1 μg/mL, and 0.1 μg/mL, respectively in B16F10 cell lines. The percentage intracellular uptake of GLY-5-FU-NEG and 5-FU-NEG was found to be 44.3 % and 53.6 %, respectively. GLY-based 5-FU-NEG formulation showed alterations in cell cycle distribution, in compared to 5-FU-NE gel. The overall findings suggest that the GLY-based 5-FU-NEG holds promise for improving anti-melanoma activity.

## 1. Introduction

Skin cancer, notably melanoma, poses a significant global health challenge. In the United States and Europe, it ranks as the most prevalent form of cancer, with nonmelanoma skin cancers (NMSCs) contributing to a substantial portion of new cases annually (Nagaraja et al., 2021). Despite representing only 1 % of skin cancers, melanoma is notoriously lethal, responsible for a considerable number of fatalities. This dichotomy underscores the urgent need for innovative therapeutic strategies (Nazir et al., 2021). Among various anticancer agents, 5-Fluorouracil (5-FU) has emerged as a prominent choice in combating skin malignancies. As an anti-metabolite, its mechanism of action centers on impeding cancer cell proliferation (Naves et al., 2017). However, conventional 5-FU formulations like Efudex, Efudix, Carac, and Fluoroplex, despite their widespread usage, exhibit significant limitations (Naves et al., 2017; Wu et al., 2021). These include poor skin permeability, limited retention at the application site, and a range of adverse dermatological reactions, often persisting for extended periods.

To address these challenges, this study proposes a novel approach: the development of a nanoemulsion-based hydrogel (NE) containing 5-FU, with glycyrrhizin (GLY) serving as a penetration enhancer (Pund et al., 2015). NEs, characterized by their biocompatibility and fluidic

* Corresponding author at: Department of Pharmaceutics, University Institute of Pharma Sciences Chandigarh University, Gharuan, Punjab, India.
*E-mail address:* dilpreet.daman@gmail.com (D. Singh).

https://doi.org/10.1016/j.jsps.2024.101999
Received 27 December 2023; Accepted 20 February 2024
Available online 24 February 2024

nature, are excellent candidates for enhancing drug loading and delivery. GLY, derived from licorice root (Glycyrrhiza glabra), has shown promising results in improving the topical delivery of active compounds. GLY, has remarkable ability not only to enhance the penetration of drugs through the skin but also for its intrinsic anti-melanoma properties (Sapra et al., 2008). This dual action positions GLY as a unique and potent agent in the fight against skin melanoma (Chen et al., 2013). Its capability to disrupt the skin's outermost barrier enhances the delivery of therapeutic agents like 5-FU directly to the target cells, while its own anti-cancer activity contributes to a synergistic effect, potentially amplifying the overall efficacy of the treatment (Chen et al., 2013; Nokhodchi et al., 2002).

The innovation of this research lies in harnessing the synergistic potential of a NE hydrogel and GLY to deliver 5-FU effectively to melanoma cells. This strategy is hypothesized not only to enhance the therapeutic efficacy of 5-FU but also to minimize its adverse effects on healthy tissues, thus offering a targeted, more efficient, and safer treatment alternative for melanoma. By bridging the gap between the need for effective melanoma treatments and the current limitations of 5-FU therapy, this study aims to contribute significantly to the field of targeted melanoma therapy. The successful development of this nanoemulgel could mark a pivotal advancement in skin cancer treatment, potentially revolutionizing the clinical approach to managing this formidable disease.

## 2. Materials and methods

### 2.1. Materials

5-FU was purchased from Himedia Pvt., Ltd. Glycyrrhizin was purchased from Yucca Enterprises, Mumbai. Tween 80 and Span 80 were purchased from CDH chemicals. Isopropyl myristate, Olive oil and Methanol have been purchased from SD Fine chemicals. Diethyl monoglycol ether (Transcutol P) was purchased from Sigma Aldrich, India. B16F10 mutine melanoma cell lines were procudred from National Centre for Cell Sciences (NCCS), Pune. Carbopol 940P, Carbapol 934 were purchased from Ranken, India. Annnexin V dye and Propidium iodide was obtained from local supplier. All chemicals and in vitro reagents were obtained from *in-house* laboratory.

### 2.2. Methods

#### 2.2.1. Screening of excipients

*2.2.1.1. Solubility studies in different excipients.* Solubility studies play a crucial role in the development of NE formulations, as they help determine the solubility of active compounds within the formulation components and guide the selection of appropriate ingredients (Zhao et al., 2021). The investigated oils were rose merry oil, oleic acid, castor oil, isopropyl myristate, vitamin E oil, and tea tree oil. Surfactants included Tween-80, Span-80, Span20, Tween-60, and Triton X100, while Co-surfactants included PEG-400, Transcutol P, and isopropyl alcohol. 2.0 ml of each lipid was added to 5.0 ml vials and 10 mg of excess of 5-FU was added and thoroughly mixed using a vortex mixer (Spinix, Mumbai India) (Al-Nima et al., 2020). Subsequently, each of the samples was centrifuged for 20 min at 5000 rpm. The concentration of 5-FU in the oils, surfactants and co-surfactants were measured at 266.0 nm using UV Vis Spectrophotometer (Shimadzu 1900i double beam UV–Visible Spectrophotometer, Japan).

*2.2.1.2. Preparation of pseudo-ternary phase diagrams.* Ternary phase diagrams for NEs can be constructed to understand the phase behavior and composition of the three main components: oil phase, aqueous phase, and surfactant/co-surfactant mixture ($S_{mix}$) (Tang et al., 2017). Oil titration method was used to develop *w/o* type NEs. On the basis of solubility experiments, three different weight ratios (1:1, 1:2 and 2:1) of Span 80: Tween80 (surfactants), and Transcutol P (co-surfactant) were developed. Afterwards, IPM was added to the mixture of surfactant: co-surfactant ($S_{mix}$) in different ratios in drop wise manner, until the formulation was transparent and clear, deionized water was eventually added. All of the pseudo-ternary phase diagrams were developed in order to identify the translucent and clear area (Nanoemulsification area). Based on the solubility of 5-FU in the water phase and the lowest amount of surfactant and cosurfactant from the every-phase diagrams, various formulations were developed. Table 1 shows the formulation chart of NE containing active drug. 5-FU (0.5 w/w, 5.0 mg/g) were incorporated in water, and an optimum proportion of surfactant and cosurfactant was additionally included with the assistance of agitation. Oil was titrated into the continuous phase to create a homogenous phase that is transparent and clear.

#### 2.2.2. Characterization of developed NE batches of 5-FU

*2.2.2.1. Thermodynamic stability tests.* On the prepared NEs, thermodynamic stability characterizations were performed, including assessments of metastable and unstable preparations. To investigate cracking, coalescence, phase separation, and creaming, all developed formulations were packed in capping vials and were centrifuged at 5000 rpm for 25 min. After exposure, the formulations were visually observed for any type of physical instability. Moreover, all formulations were exposed to heating and cooling cycles. Three cycles were performed between temperatures of 4.0 °C and 45.0 °C, and samples were stored for 48 h at each temperature. These formulations were also subjected to freeze thaw cycling at −21.0 ± 0.50 °C to 20.0 ± 0.50 °C for 24 h. Formulations were selected based on their physical stability during the heating and cooling cycles. Only the thermodynamically stable preparations were retained for further characterization and evaluation (Quan et al., 2021).

*2.2.2.2. Globule size and PDI analysis.* Developed nanoemulsion batches were characterized in terms of globule size, polydispersity index (PDI), drug content, and percentage transmittance. Using a particle size analyser (Beckman Coulter, Delsa Nano C, USA), the polydispersity index (PDI) and mean globule size of the developed nano emulsion were determined. By measuring the variations in laser light intensity scattered by particles as they diffuse through a fluid, the analyzer uses photon correlation spectroscopy (PCS), which enables the estimation of particle size. (Quan et al., 2021). A 3 ml sample of the NE was placed in a cuvette for particle size and PDI in a back scattering mode. The absence of bubbles allowed accurate measurements to be obtained (Beiu et al., 2020).

*2.2.2.3. Drug content and percentage transmittance analysis.* All batches of stable nanoemulsions were tested for drug content. To get the necessary drug concentration, nanoemulsion was diluted (1 ml ofNE was diluted up to 10 ml) with methanol. Absorbance was measured using a UV spectrophotometer (Shimadzu 1900i double beam UV–Visible Spectrophotometer, Japan) at 266 nm (Al-Nima et al., 2020). The drug

**Table 1**
Composition chart of various nanoemulsions based 5-FU formulations.

| Batch code | Oil (IPM) (%w/w) | Surfactant (Span80: Tween 80) (1:1) (%w/w) | Co–surfactant (Transcutol-P) (%w/w) | Water (Deionized Water) (%w/w) | Smix ratio |
|---|---|---|---|---|---|
| NE-1 | 50 | 20 | 20 | 10 | 1:1 |
| NE-2 | 40 | 22.5 | 22.5 | 15 | 1:1 |
| NE-3 | 30 | 25 | 25 | 20 | 1:1 |
| NE-4 | 50 | 13 | 26 | 10 | 1:2 |
| NE-5 | 40 | 15 | 30 | 15 | 1:2 |
| NE-6 | 30 | 17 | 33 | 20 | 1:2 |
| NE-7 | 50 | 26 | 13 | 10 | 2:1 |
| NE-8 | 40 | 30 | 15 | 15 | 2:1 |
| NE-9 | 30 | 33 | 17 | 20 | 2:1 |

content of optimized formulation was calculated on the basis of given formulae (1).

$$Initialdrugconcentration - finaldrugconcentration/initialdrugconcentration*100 \quad (1)$$

Moreover, all the developed 5-FU loaded NE batches was done to check the optical clarity of formulation and the transmittance was calculated by taking water as a standard in a U.V. spectrophotometer at 538 nm (Beiu et al., 2020).

*2.2.2.4. Transmission electron microscopy.* The morphology of the optimized 5-FU NE was examined using a High resolution electron microscope (HRTEM 2100 Plus, Joel, Japan). A drop of the formulation dispersion was placed on a carbon-coated copper grid and allowed to air dry for 15 min. The sample was then stained with a 1 % w/v phosphotungstic acid solution and excess stain was removed The dried samples on a grid was visualized using the software at different magnifications (Beiu et al., 2020).

*2.2.3. Development of GLY-based 5-FU NE-based gel*

Nanoemulgel (NEG) containing Gly-based 5-FU NE was prepared using the different concentrations of 0.5, 1, and 1.5 % Carbopol 940P gel base. The appropriate concentrations of gel base were prepared by accurately weighed Carbopol 940P and mix with water through mechanical shaker at 1500 rpm for 30 min. The gel base was then kept aside 24 h in the dark background for swelling. GLY, as a penetration enhancer (0.1 % *w/w*, 1 mg/g) was added in optimized NE formula and dispersed in prepared gel bases to obtain GLY-5FU-NEG (Nokhodchi et al., 2002; Madni et al., 2018). The concentration of 0.1 % w/w was chosen based on studies indicating its effectiveness at low concentrations without causing skin irritation or toxicity (Beiu et al., 2020; Madni et al., 2018). Triethanolamine was added in optimum quantity to maintain the pH of gel preparation. The final batch chart of different concentrations of carbopol prepared GLY based 5-FU NEG was depicted in Table 4.

*2.2.3.1. Characterization of GLY-Based 5-FU NE gel.* .

*2.2.3.2. Homogeneity and pH.* The homogeneity of the prepared optimized GLY-based 5-FU Nanoemulgel with three different carbopol concentrations was assessed through visual inspection in the container. For pH assessment, 1 g sample of the formulation was diluted with 10 ml of water and thoroughly shaken. The apparent pH of the diluted formulation was measured in triplicate at 25 ± 1 °C using a digital pH meter (Mettler Toledo, Japan) equipped with a glass microelectrode. The pH meter was allowed to equilibrate for 1 min prior to measurement (Madamsetty et al., 2020).

*2.2.3.3. Spreadability.* The spreadability of the gel was evaluated by slide drag method. A modified apparatus consisting of two glass slides was used for the evaluation. The upper slide was attached to a balance using a hook, while the lower slide was fixed to a wooden plate. The upper plate was weighted with 100 g, and a sample of the gel (1 g) was placed between the two glass slides. The change in spreading diameter resulting from the application of weight to spread the gel was observed (n = 3). The spreadability was calculated using the following formula (2)

$$S = W*L/t \quad (2)$$

where W is the weight in a pan (gm), 'L' is the fixed length moved by the glass slide, S represents the spreadability (g/sec), and 't' is the time (sec) required to separate the slides (Madni et al., 2018; Madamsetty et al., 2020).

*2.2.3.4. Texture analysis.* The texture of the optimised GLY-based 5-FU NEG was analysed using the automated CT3 Texture Analyzer (Brookfield Engineering Laboratories, USA) by TA15/100 spindle hood. Sample was placed in sample array tray and spindle hood was dipped in sample. The force required to break the gel was recorded. The hardness, firmness and adhesiveness was performed in triplicate and calculated. (Nicoli et al., 2008).

*2.2.3.5. Rheological analysis.* The rheological behavior of the microemulsion based gel system was studied using calibrated rheometer (Anton Paar Rheolab, USA). The viscosity of optimized GLY-5FU NEG gel was measured using spindle no. 5 and visocity was determined at a constant shear rate under ambient temperature.

*2.2.3.6. Thermal analysis.* DSC analysis of 5 FU, 5-FU NEG and GLY-5FU-NEGwas carried out using a DSC instrument (Perkin Elmer 6000, Pyris). Each sample was sealed in a small aluminium pan and scanned in the range 30—350 °C at 20 °C heating rate. The empty pan was used as a reference standard and inert nitrogen gas was inserted at a flow rate of 60 ml/min till completion of the experiment (Farhana, 2023).

*2.2.4. In-vitro drug release study*

The *in-vitro* drug release of 5-FU gel, 5-FU NEG and GLY-5FU-NEGGLY-5FU-NEGwas determined using a modified USP Type II dissolution apparatus (Lab India, DS 8000, India), which was equipped with 200 ml glass vessel and enhancer cells (PSENHANC-040 Enhancer cell 4 $cm^2$ surface area membrane). The enhancer cell assembly procedure involved loading the testing samples into the enhancer cells and fitted with a dialysis membrane (MWCO 12 kDa) backed by a hollow circular plate exposing a 2 $cm^2$ membrane area to the dissolution medium. The assembled enhancer cell was then gently placed into the glass vessel. The release medium utilized was phosphate buffer (pH 7.4) and volume was 200 ml which poured into the glass vessel. The entire assembly was subjected to constant stirring at 50 rpm and maintained at a temperature of 37 ± 0.5 °C. At predetermined time intervals (15, 30, 60, 120, 240, 480, 720, 1020, and 1440 min), an aliquot of the release media was withdrawn and replaced with fresh media to maintain the sink condition. The withdrawn samples were analyzed using UV–visible spectrophotometry at 266 nm to determine the amount of 5-FU released in tested formulations. The experiment was performed in triplicate and comparative graphs were plotted (Simon et al., 2016).

*2.2.5. Ex vivo permeation study*

The ex-*vivo* skin permeation study was conducted using freshly excised pig skin which was obtained from a local slaughter house. Pig skin was chosen due to its histological similarity to human skin, with the stratum corneum of pig pinna having a thickness of 21–26 μm and an average of 20 hair follicles (Ayub et al., 2007). Moreover, pig skin is readily available and widely used in skin permeation studies, making it the preferred model for this study. The *ex-vivo* permeation of 5-FU gel, 5-FU-NEG and GLY-5FU-NEGGLY-5FU-NEGwas determined using a modified USP Dissolution Apparatus equipped with 200 ml glass vessels and enhancer cells. The dorsal portion of pig ear skin was shaved using a hair clipper, and subcutaneous fat was removed. The skin samples were shaved and prepared to expose the outer layer (epidermis) to the formulations while maintaining the inner layer (dermis) facing the dissolution medium (Ayub et al., 2007). The skin was then washed thrice with PBS (pH 7.4). Samples were loaded into the enhancer cells which were

then gently placed into the glass vessel filled with phosphate buffer (pH 7.4). The entire assembly was subjected to constant stirring at 50 rpm and maintained at a temperature of 37 ± 0.5 °C. At predetermined time intervals (15, 30, 60, 120, 240, 480, 720, 1080, and 1440 min), an aliquot of the release media was withdrawn and replaced with fresh media. The concentration of the drug in the samples was analyzed using UV–visible spectrophotometry. The permeation rate of 5-FU through the skin was calculated by plotting the cumulative amount permeated per unit area against time. (Ayub et al., 2007; Monge-Fuentes et al., 2014). The permeability parameters including permeability coefficient (kp), steady state flux ($J_{ss}$) and enhancement ratio (Er) was calculated as per standard methodologies.

#### 2.2.6. Cell lines studies using B16F10 melanoma cell lines

*2.2.6.1. Cytotoxicity assessment and intracellular uptake.* B16F10 cell lines, a well-established murine melanoma cell lines were procured from National Centre for Cell Science (NCCS) Pune which was utilized as a passage number ranging from 5 to 10 (Chen and Zhang, 2016). Cells were thawed and cultured in cell culture medium i.e. Dulbecco's Modified Eagle Medium (DMEM) supplemented with 10 % fetal bovine serum and 1 % penicillin–streptomycin (Chen and Zhang, 2016). Afterwards, maintain the cells in a controlled environment (37 °C, 5 % $CO_2$) and passage them regularly to maintain cell viability and growth. The cells were seeded by preparing the required number of multi-well plates and seeded into the wells at a desired density. Incubate the plates in the cell culture incubator for a sufficient time period to allow the cells to attach and form a monolayer for 24 h. Samples were divided into 3 groups Group A consisted of Pure 5-FU in gel base, Group B consisted of 5-FU NEG and Group C consisted of GLY-5-FU NEG and concentrations was taken at 0.1–10 µg/ml. Afterwards, the test compounds were added to the respective wells containing the seeded B16F10 cells. Include appropriate controls (e.g., untreated control) for comparison. After incubation, the cell cytotoxicity and the $IC_{50}$ value of the formulation were calculated (Chen and Zhang, 2016; Rigon et al., 2015).

*2.2.6.2. Cell cycle analysis.* For cell cycle analysis, carefully aspirate the medium from the culture dish and rinse the cells once with PBS to remove residual medium and detached cells. Add an appropriate volume of trypsin-EDTA solution to cover the cells and incubate for a few min at 37 °C. Centrifuge the cell suspension at a low speed (e.g., 300–500 × g) for 5 min to pellet the cells. Afterwards, fix the cells by adding cold 70 % ethanol drop wise to the cell pellet while gently vortexing or swirling the tube and incubate the fixed cells at 4 °C for at least 30 min or overnight. After incubation, staining with propidium iodide has been done for staining of DNA. The treated cells were analyzed for flow cytometry for PI detection and the desired fluorochromes used in the experiment (Raju et al., 2017). For gating in different cell phases i.e. G0/G1 Phase Cells which Identified by their single DNA content, representing cells that are either in a quiescent state (G0) or in the initial phase of the cell cycle (G1). S Phase Cells which characterized by varying levels of DNA content due to ongoing DNA replication and last phase is G2/M Phase Cells which distinguished by their double DNA content, indicating cells that are either preparing for or are in the process of cell division. The data was collected on the DNA content of the cells using appropriate gating strategies to distinguish cell cycle phases (G0/G1, S, G2/M). The data was analyzed using flow cytometry analysis software to determine the distribution of cells in different cell cycle phase (Raju et al., 2017).

*2.2.6.3. Intracellular uptake study.* The intracellular uptake of Rhodamine loaded 5-FU gel was determined in B16F10 cells in comparison with the Rho-FU-NE (Rhodamine and 5-FU co-loaded NE) and Rho-FU NEG (Rhodamine and 5-FU-GLY co-loaded NEG) formulation. The formulation was prepared by loading Rhodamine B dye (Practical Grade Himedia Labs, India) into the formulation in a similar manner during the production of NE preparation. The B16 F10 cells were seeded in 96 well plates at 37 °C for 24 h followed by treating the cells. Post-treatment, the cells were trypsinized to detach them from the well plates. The intracellular uptake of the test samples were analysed by the B16F10 cells was then quantitatively analyzed using an Elisa Reader, specifically measuring absorbance at a wavelength of 643.5 nm. This method ensures a standardized approach to evaluate and compared the efficacy of each NE based formulations in terms of their cellular uptake efficiency (Sack et al., 2014).

### 2.3. Statistical analysis

Statistical analysis of multiple parameters was conducted using Origin Software, version 8.5.1 (Northampton, USA). One-way ANOVA was utilized at a confidence level of 95 % ($p < 0.05$) to assess the statistical significance and reproducibility of the proposed method.

## 3. Results

### 3.1. Solubility study

According to the results obtained, 5-FU showed maximum solubility was observed in lipophilic surfactant Span 80. In order to encapsulate maximum drug loading, a prototype hydrophilic surfactant was added along with Span 80. Solubility results observed Tween 80 demarcated maximum solubility of 8.6 mg/g. When formulating and developing NE, short chain alcohols type co-surfactants are thought to be safe for pharmaceutical therapeutic applications and are well compatible with surfactants. Among the co-surfactants/co-solvents tried, maximum solubility was observed in Transcutol P. Hence IPM, Span 80, Tween 80 and Transcutol P were used as oil, surfactant and co-surfactant for further studies. Fig. 1 provide the compiled solubility data of 5-FU in various oils, surfactants and co-surfactants.

### 3.2. Construction of pseudo-ternary phase diagrams

Pseudo ternary phase diagrams were constructed for three ratios viz. 1:1, 1:2, 2:1 of Surfactant: Co-surfactant mix ($S_{mix}$). From the three plotted phase diagrams, an equal propionate of nanoemulsification region was found to be in all ratios, respectively. However, the largest microemulsion region was observed in the NE containing 1:1 ratio of $S_{mix}$. It was observed from the pseudo ternary phase diagrams obtained, that an equal concentration in the surfactant concentration and co-surfactant concentration (1:1 ratio) exhibits NE region larger in comparison to other phase diagrams (Fig. 2a-c). The collective Area under the microemulsion region (AMR) was found to be 45.32, 47.32 and 46.23, respectively. From the observations gathered, the AMR is almost equal in propionate with each $S_{mix}$ ratio and further selected for formulation studies.

### 3.3. Characterization of developed NE batches of 5-FU

#### 3.3.1. Thermodynamic stability tests

NEs were stored at different temperature like −21 °C to 4 °C for not less than 48 h at each temperature. The results observed that satisfactory stability was exhibited as they remained transparent and no creaming, precipitation or phase separation was observed in developed formulations (Table 2).

#### 3.3.2. Percentage transmittance and drug content

5-FU-loaded NEs were evaluated for percent transmittance and obtained results are shown in Table 3. The evaluated formulations exhibited satisfactory transparency as expressed by the transmittance values which is desired for good nanoemulsion properties. NE is characterized by optimum clarity and stability which might be due to the

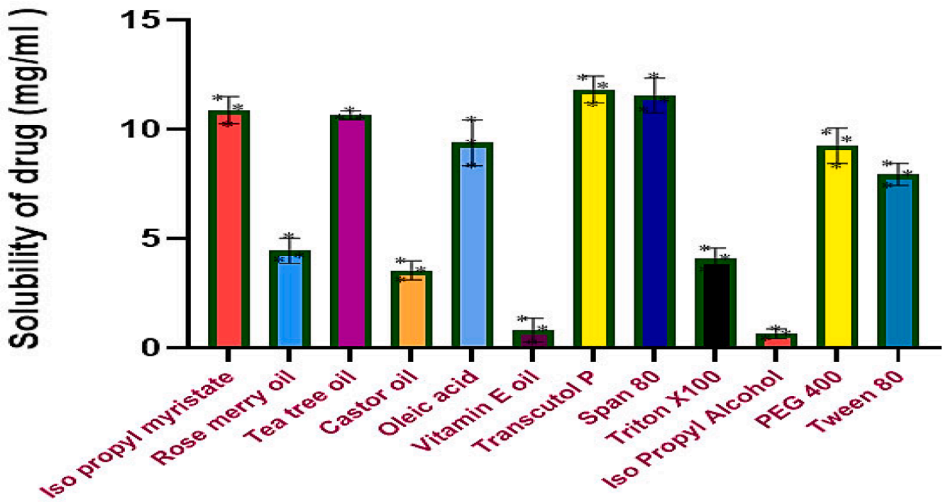


**Fig. 1.** Solubility studies of 5-FU indifferent lipid excipients viz. oil, surfactant and co-surfactant (n = 3, SD).

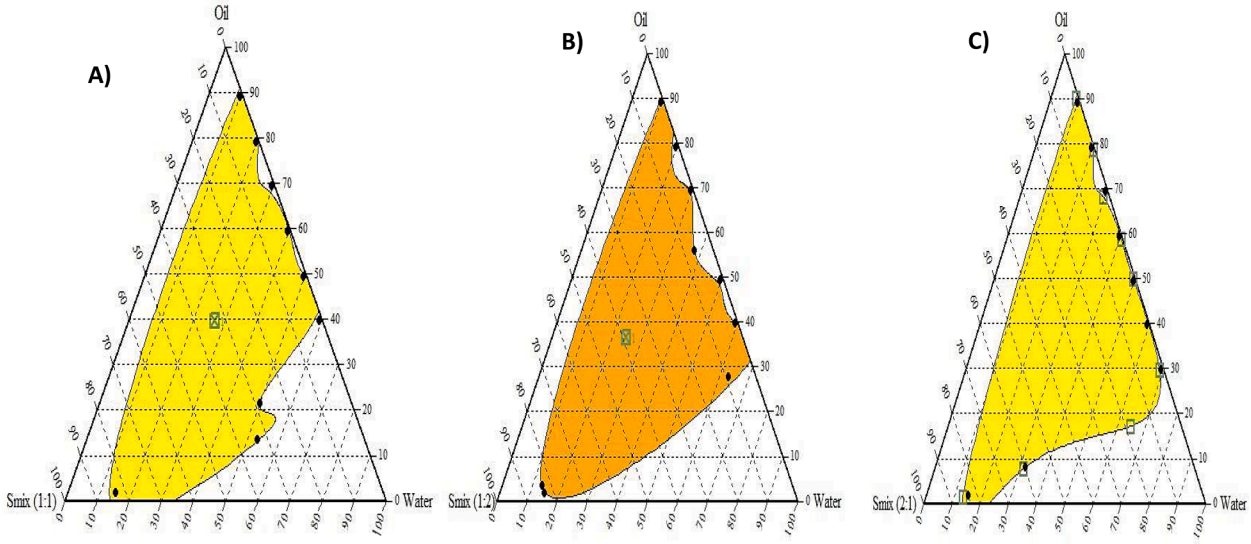


**Fig. 2.** Evaluation of zones of nanoemulsions by pseudo ternary phase diagrams on the basis of various concentrations of Smix ratios of A) 1:1, B) 1:2 and C) 2:1.

**Table 2**
Thermodynamic Stability of prepared batches of nanoemulsion based 5-FU formulations.

| Batch Code | Thermodynamic Stability Studies | | |
|---|---|---|---|
| | Centrifugation Test | Heating Cooling Cycle | Freeze-Thaw cycle |
| NE-1 | – | – | – |
| NE-2 | + | + | + |
| NE-3 | – | – | – |
| NE-4 | + | + | – |
| NE-5 | + | + | + |
| NE-6 | + | + | + |
| NE-7 | + | + | + |
| NE-8 | + | + | + |
| NE-9 | + | + | + |

compatibility between $S_{mix}$ and oil phase that form an isotropic and spontaneous system exhibiting optimum clarity. Regarding highest drug content was observed in F8 formulation i.e. 97.32 %. Hence, the results were satisfactory and further optimized for particle size and PDI analysis.

**Table 3**
*In-vitro* characterization of prepared nanoemulsion based batches of 5-FU formulations.

| Batch code | Globule Size (nm) | PDI | Drug Content (%) | % Transmittance |
|---|---|---|---|---|
| NE-1 | 164.2 ± 8.21 | 0.312 ± 0.02 | 89.6 ± 6.27 | 87.4 ± 12.23 |
| NE-2 | 114.5 ± 6.87 | 0.278 ± 0.02 | 85.4 ± 7.68 | 91.3 ± 4.56 |
| NE-3 | 108.2 ± 6.49 | 0.431 ± 0.03 | 82.1 ± 5.74 | 95.4 ± 6.67 |
| NE-4 | 239.1 ± 7.17 | 0.284 ± 0.01 | 83.6 ± 5.85 | 84.5 ± 7.60 |
| NE-5 | 171.7 ± 13.73 | 0.239 ± 0.02 | 81.5 ± 7.33 | 86.9 ± 6.08 |
| NE-6 | 156.1 ± 7.80 | 0.27 ± 0.010 | 78.8 ± 3.15 | 83.6 ± 5.85 |
| NE-7 | 93.0 ± 7.44 | 0.385 ± 0.03 | 92.5 ± 8.32 | 93.2 ± 8.38 |
| NE-8 | 64.1 ± 5.12 | 0.196 ± 0.01 | 97.3 ± 5.83 | 98.8 ± 10.86 |
| NE-9 | 109.3 ± 7.65 | 0.34 ± 0.04 | 94.4 ± 11.32 | 96.4 ± 11.56 |

**Table 4**
*In house* characterization parameters of prepared GLY-5-FU NEG formulations.

| Gel batch | Visual appearance | pH | Spreadability (g. cm) |
|---|---|---|---|
| **Carbapol 940 (0.5 %w/w)** | Less Viscous | 7.3 ± 0.56 | 18.2 ± 0.98 |
| **Carbapol 940 (1.0 % w/w)** | Consistency Poor | 6.9 ± 0.53 | 22.3 ± 1.06 |
| **Carbapol 940 (1.5 % w/w)** | Good Consistency | 6.7 ± 0.49 | 26.4 ± 1.12 |

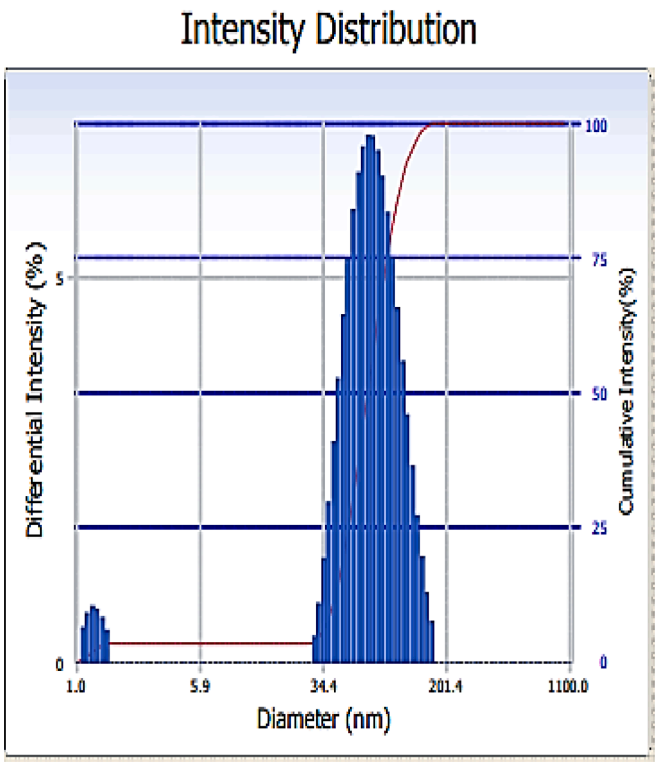


**Fig. 3.** Globule size distribution of optimized NE formulation (F-8).

### 3.3.3. *Globule size and PDI analysis*

Table 3 depicts the average particle size and PDI of formulation batches of F1-F9. The average particle size range of the optimized NE1 to NE9 was ranged from 64.1 ± 5.1 to 239.1 ± 7.1 nm, respectively. The optimized NE-8 has the desired attributes of an ideal NE formulation and observed with a size range of 64.1 nm (Fig. 3). The average PDI of F1-F9 formulations were observed in a range of 0.196 ± 0.011–0.431 ± 0.036, respectively for all the developed formulations. These results indicated fairly stable and nanometric nature of nanoemulsions was observed.

### 3.3.4. *Transmission electron microscopy*

High-Resolution Transmission Electron Microscopy (HRTEM) was used to examine the morphological properties of prepared GLY-5FU-NEG. The TEM revealed a well-defined, spherical structure of nano-emulsion globules with homogeneous outer surfaces. The developed NE globules indicated with negligible coalescence and no drug precipitation was observed (Fig. 4).

### 3.3.5. *Evaluation of GLY-based nanoemulgel*

The developed GLY-based 5-FU NEG with different 3 different carbopol concentrations of 0.5 % *w/w*, 1 % *w/w* and 1.5 % *w/w* was characterized for various physical parameters and results are shown in Table 4. The gel formulation with carbopol concentration of 1.5 % *w/w* was selected as an optimized formulation due to its good visual

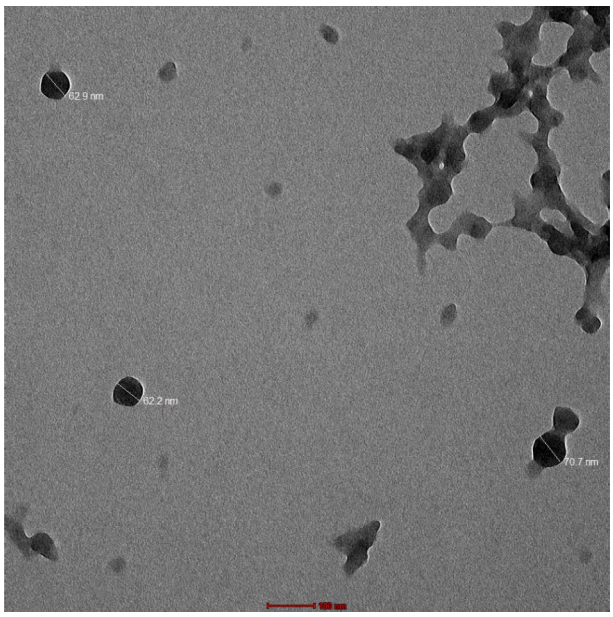

**Fig. 4.** TEM micrograph of Optimized nanoemulsion formulation of 5-FU.

appearance, pH and spreadability. The optimized gel formulation had a smooth, uniform appearance and was free of roughness. The optimized formulated topical gel's pH was found to be 6.7 ± 0.49, which is considered to be an acceptable level to prevent the possibility of skin irritation when applied to the skin. Spreadability aids in a uniform application at the site and plays a significant role in patient compliance and was found to be 26.4 ± 1.12 g.cm. Moreover, the viscosity of optimized gel was performed and was found to be 2763 cP.

*3.3.5.1. Texture analysis.* The optimized formulation of GLY-5FU-NEG was evaluated for texture analysis and the parameters such as adhesiveness, springiness, deformation of hardness and adhesiveness force were evaluated and the results obtained are shown in Table 5 and graph is shown in Fig. 5.

*3.3.5.2. Differential scanning calorimetric analysis.* DSC investigation was used to examine the variations in thermal behaviour for 5-FU, 5-FU-NEG, and GLY-5FU-NEG. Thermal behavior of 5-FU revealed a distinct endothermic peak with a sharp peak at 302.2 °C, suggesting the drug's crystalline state. In both gels, the peak shifted to 162.3 °C. The lack of the 5-FU endothermic peak in the nanoemulgel formulation may be a sign that the drug is trapped inside the gel. The results are shown in Fig. 6.

*3.3.5.3. In vitro drug release studies. In-vitro* drug release of 5-FU gel, 5-FU NEG, and GLY-5FU-NEG were performed. 5-FU gel showed 100 % drug release within 12 h. 5-FU NEG showed 85.79 % drug release within 24 h and GLY-5FU-NEG showed 74.11 % drug release within 24 h. Finally, the optimized GLY-5FU-NEG released 20.41 ± 1.88 % in initial 2 h, which showed an initial burst release and after that showed sustained release pattern till 24 h (Fig. 7). Due to the eroding outer layer of 5-FU in both gels, 5-FU burst release was depicted in optimized GLY-

**Table 5**
Characterization of optimised GLY based 5-FU-NEG by texture analysis.

| Parameter's | Result |
|---|---|
| Adhesiveness (mJ) | 0.6 ± 0.01 |
| Springiness (n) | 0.092 ± 0.002 |
| Deformation of hardness (cm) | 0.21 ± 0.005 |
| Adhesiveness force (N) | 0.06 ± 0.007 |

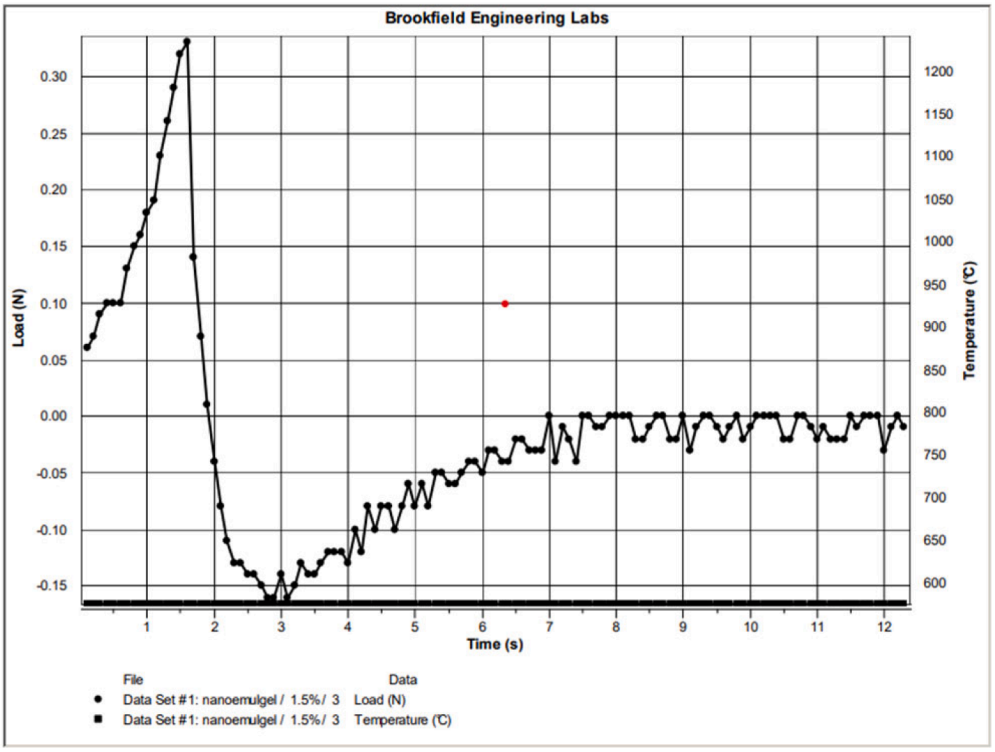


**Fig. 5.** Texture analysis of optimized GLY- 5-FU NEG formulation.

5FU-NEGGLY-5FU-NEG and optimized-5-FU-NEG When optimized GLY-based 5-FU-NEG was allowed to fit in the numerous kinetics models, the greatest value for $R^2$ was fit to the high standard release models (in vitro) for 5-FU. The highest value matched to the First order, $R^2 = 0.974$. The value of ($R^2$) of Higuchi nmodel was discovered to be 0.9443, followed by zero order ($R^2 = 0.9555$) and Korsmeyer-Peppas ($R^2 = 0.686$).

*3.3.5.4. Ex-vivo skin permeation studies.* To compare the drug permeation rate of optimized 5-FU gel, 5-FU NEG, and GLY-5-FU-NEG, *ex vivo* skin permeation investigations were executed. The curve was plotted between cumulative 5-FU permeation and time (h) to determine permeability parameters such as $J_{ss}$, $k_p$, and Er. The rate of *ex vivo* skin penetration was highest in the GLY-based 5-FU NEG formulation and lowest in the 5-FU gel as depicted in Fig. 8. When compared to 5-FU gel and other formulations, the skin penetration profile of GLY-based 5-FU NEG was determined to be notably significant, as compared to 5-FU-NEG and Plain 5-FU gel. The values for the above mentioned parameters for the three tested formulations are shown in Table 6. Jss, Kp and Er values for optimized formulation were found to be 9.109, 2.898 and 4.871, respectively.

*3.3.6. In vitro cell line study*

*3.3.6.1. Cytotoxicity assessment.* The cytotoxicity of GLY-NE-5-FU was compared with NE, and 5-FU was assessed in B16F10 cell lines via MTT assay. The cells were cultured in different concentrations (0.1–10 μg/ml) of both formulations and drug. It was observed that the high cytotoxicity was observed at lower drug concentrations with GLY based 5-FU NEG formulation followed by 5-FU Gel as illustrated in Fig. 9. Whereas, pure 5-FU at requires high concentration to produce the same cytotoxicity as shown by both the liposomal formulation. The $IC_{50}$ value of Plain 5-FU gel, 5-FU-NEG and GLY-5FU-NEGGLY-5FU-NEGwas found to be 20, 1.1 and 0.1 μg/ml, respectively. These results indicate that GLY-5FU-NEG required a much lower concentration than NE and plain Gel to kill the same number of melanoma cells.

*3.3.6.2. Intracellular uptake study.* The intracellular uptake of the formulation was determined by loading Rhodamine-B into both NE based formulations (5-FU-NEG and GLY-5-FU-NEG) and the uptake was checked by comparing the fluorescence intensity of the tested formulations. The results depicting that the GLY-5-FU-NEG showed higher fluorescence intensity in comparison to 5-FU-NEG as shown in Table 7. The percentage intracellular uptake of GLY-5-FU-NEG and 5-FU-NEG was found to be 44.3 and 53.6, respectively.

*3.3.6.3. Cell cycle analysis.* The results demonstrated significant alterations in the cell cycle profile, suggesting potential effects of the developed formulations on cell cycle progression in B16F10 melanoma cells. The observed changes in the B16F10 melanoma cells' cell cycle distribution indicated that the GLY-5FU-NEG formulation may have the ability to affect cell cycle progression. The decrease in the percentage of cells in the G0/G1 phase indicates a possible disruption of the cell cycle arrest, while the increase in the proportion of cells in the S and G2/M phases suggests enhanced cell cycle progression or delayed cell cycle transition in the optimized formulation, as compared to 5-FU-NE gel (Table 8).

## 4. Discussion

As nanoemulsions (NEs) have high drug loading and a high drug solubilizing capacity, they can overcome stratum corneum barrier and partition the drug into the skin (de Moura et al., 2021). Solubility of 5-FU was estimated in various oils, surfactants and co-surfactants / cosolvents.. In this present study, solubility of the chosen actives was found to be highest in IPM amongst all the tried oil components for 5-fU solubility. As an oil component, IPM assists in enhancing the permeation of 5-FU through the skin barrier. Its ability to interact with the stratum corneum lipids and disrupt the skin's barrier function promotes deeper penetration of the drug, enhancing its bioavailability at the site of action (de Moura et al., 2021). IPM contributes to the physical stability of the NE by providing a suitable medium for the dispersion of surfactants and co-surfactants. Its compatibility with the other formulation components

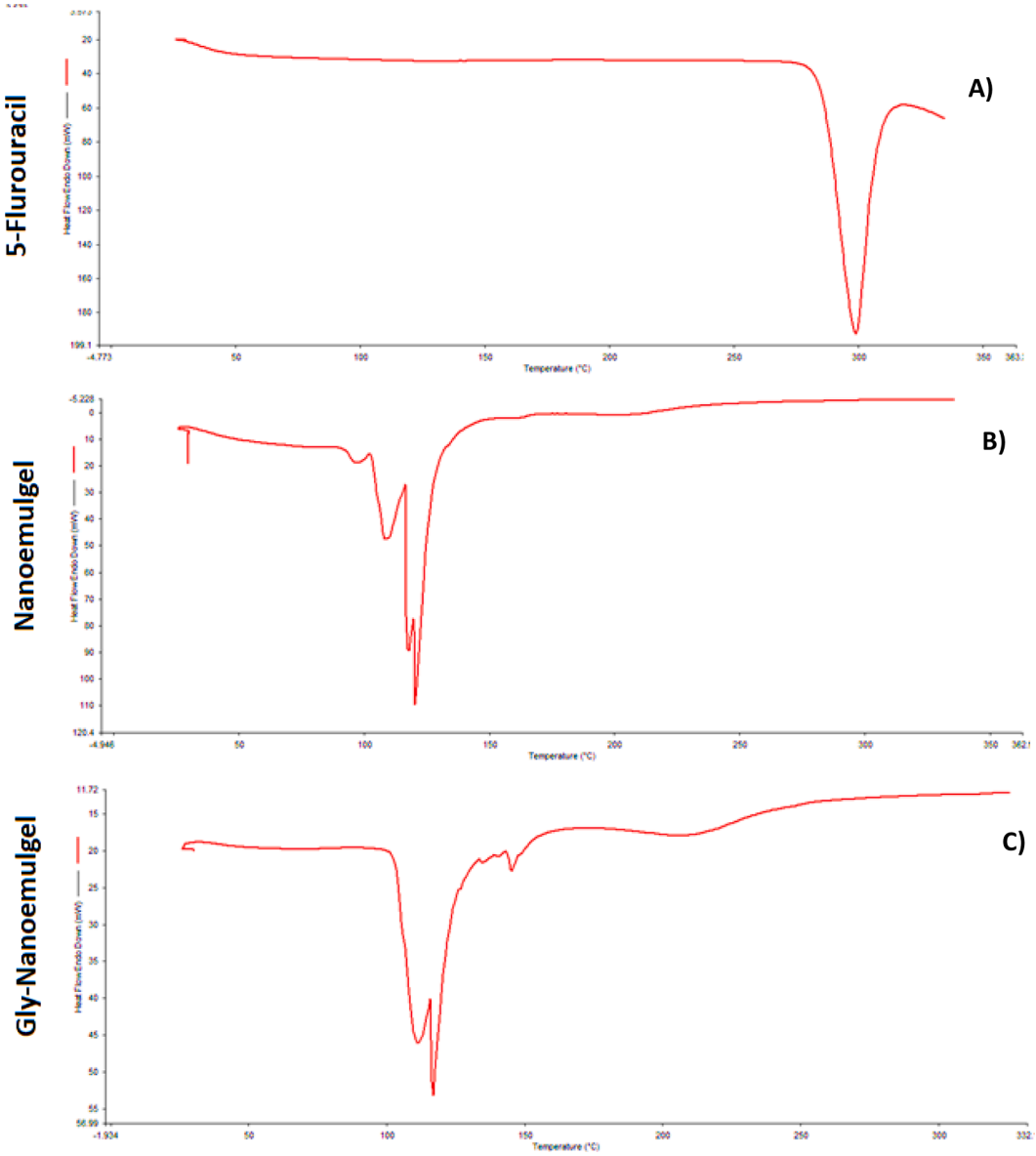


**Fig. 6.** DSC graphs of A) pure 5FU, B) optimized 5FUNEG and C) Gly-5FU NEG.

helps prevent phase separation and maintains the nanometric size of the emulsion droplets (Pinho et al., 2019). The most crucial factor for creating a nanoemulsion is based on the surfactants and their toxicity (Pinho et al., 2019; Madamsetty et al., 2020). A large amount of surfactant delivered transdermal may irritate the skin. According to earlier reports, non-ionic surfactants are safer than ionic surfactants. Span 80 (sorbitan monooleate) is a non-ionic surfactant known for its excellent emulsifying properties in oil-in-water (o/w) emulsions, contributing to the stability of the system (Hartmann et al., 2022). Tween 80 (polysorbate 80), another non-ionic surfactant, was chosen for its ability to reduce surface tension significantly, thereby enhancing the emulsion's permeability and spreadability on the skin. Its compatibility with Span 80 is particularly beneficial in forming a stable interface, crucial for the integrity of the NE (Hartmann et al., 2022; Farhana, 2023). Co-surfactants are selected on the basis of compatibility and strong interfacial tension reduction ability 30]. Transcutol P (diethylene glycol monoethyl ether), known for its excellent solubilizing capacity, serves as a co-surfactant and penetration enhancer (Monge-Fuentes et al., 2014). It facilitates the incorporation of both hydrophilic and lipophilic drugs, making it ideal for our GLY based NEG formulation. According to the final results, IPM was selected as a oil phase, Tween 80:Span 80 was selected as a $S_{mix}$ and Transcutol P was selected as co-surfactant respectively (Chen and Zhang, 2016). Ternary phase diagram involving IPM, Tween 80: Span 80, and Transcutol P can provide valuable insights into the formulation of stable NE or dispersed systems (Chen and Zhang, 2016). These diagrams are instrumental in identifying the regions where stable emulsions are formed, guiding the optimization of component ratios for effective NE formulations (Rigon et al., 2015). Our results highlight that 1:1, 1:2 and 2:1 ratio of surfactant blend (Tween 80 and Span 80) to co-surfactant (Transcutol P) within the emulsion region was found to be the most effective. This optimized ratio contributes to the stability, appearance, and performance of the NE system. The 1:1 ratio ensures a delicate balance between surfactant and co-surfactant, enhancing the system's ability to solubilize the drug effectively (Raju et al., 2017). This synergy enhances the reduction of surface tension at the oil–water interface, leading to the formation of a more stable and homogenous NE. Hence, all three rations was selected for optimization studies (Raju et al., 2017). The characterization of developed nanoemulsion (NE) batches of 5-FU involves a series of tests aimed at evaluating various aspects of the formulation's stability, drug

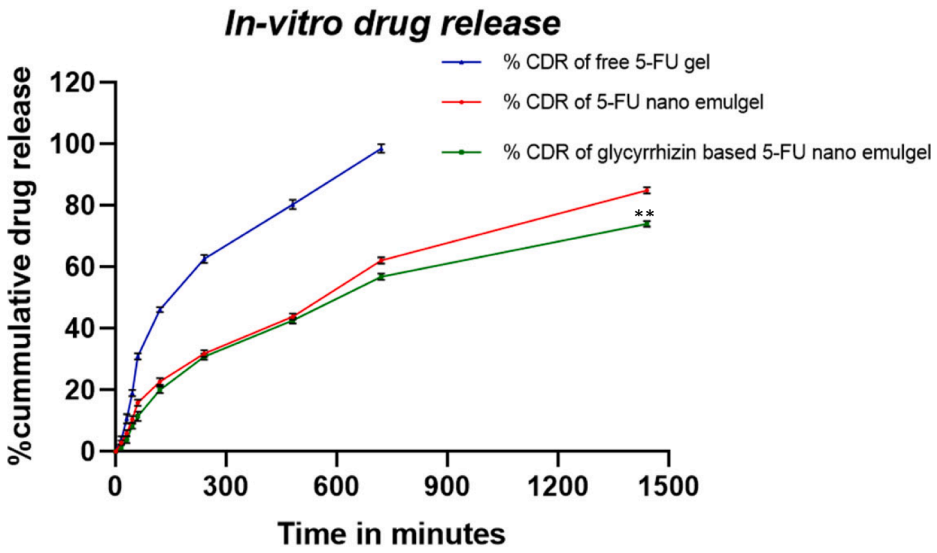


**Fig. 7.** *In vitro* release profile of 5FU, 5FU NEG and Gly-5FU-NEG in PBS7.4 using dialysis bag method [Mean ± SD, n = 3] $^{**}p < 0.05$, compared with pure 5FU gel.

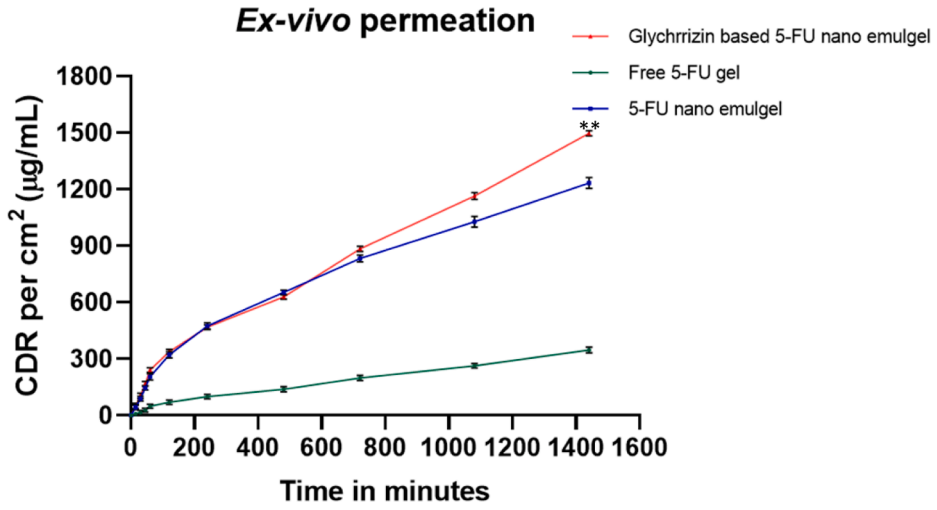


**Fig. 8.** *Ex-vivo* permeation study of 5-FU Gel, 5-FU-NEG, GLY- 5-FU NEG (n = 3, Mean ± SD), $^{**}p < 0.05$, compared with pure 5FU gel.

**Table 6**
Data analysis of permeation profile of standard and optimized gel batches.

| Batch Code | Jss (µg/cm$^2$/h) | Kp (cm/h) | Er |
|---|---|---|---|
| **5-FU Gel** | 1.873 ± 0.002 | 0.595 ± 0.003 | 1.000 ± 0.001 |
| **5- FU NEG** | 7.212 ± 0.005 | 2.294 ± 0.027 | 3.855 ± 0.004 |
| **GLY-5- FU NEG** | 9.109 ± 0.007$^{**}$ | 2.898 ± 0.65$^{**}$ | 4.871 ± 0.036$^{**}$ |

$^{**}p < 0.05$, compared with 5FU gel.

content, particle size, and morphology. Each test provides unique insights into the behavior of the NE system and its potential for pharmaceutical application. Thermodynamic stability tests, such as centrifugation and freeze–thaw cycles, are essential to assess the formulation's robustness against phase separation under stress conditions (Sack et al., 2014). A stable NE should ideally withstand these challenges, maintaining a homogeneous distribution of phases (De Moura et al., 2021). Favorable results from these tests indicate that the chosen combination of surfactants, co-surfactants, and oil phase is effective in preventing phase separation, ensuring consistent drug delivery and application. The measurement of percentage transmittance provides insights into the clarity and transparency of the NE (Pinho et al., 2019). Higher transmittance value of developed formulations (NE-8) indicates minimal light scattering due to uniform droplet size distribution. Simultaneously, the evaluation of drug content ensures that the intended amount of the active pharmaceutical ingredient (5-FU) is encapsulated within the nanoemulsion. High drug loading in NE-8 i.e. 97.32 suggest successful incorporation of the drug, and high transmittance points toward the NE's visual appeal and potential for efficient drug delivery (Kanugo, 2022). Globule size and PDI analysis are crucial for assessing the physical stability and homogeneity of the nanoemulsion. A low PDI indicates a narrow size distribution of droplets, while a smaller globule size generally enhances bioavailability due to increased surface area (Arasi et al., 2020; Running et al., 2018). Favorable results in these analyses suggest that the formulation is uniform, with consistent droplet sizes, which can improve the solubilization of hydrophobic drugs like 5-FU, leading to enhanced drug release and potential therapeutic efficacy. TEM provides high-resolution images of the nanoemulsion structure, allowing direct observation of droplet morphology and interactions (Wang and Chang, 2021). TEM can reveal insights into the arrangement of droplets, micellar structures, and potential interactions with the drug (Liu et al., 2017). The homogeneity and integrity of these globules are crucial for several reasons. First, the spherical shape and uniformity suggest efficient packing of the surfactants at the oil–water interface, which is essential for maintaining the stability of the NE. Stable NE are

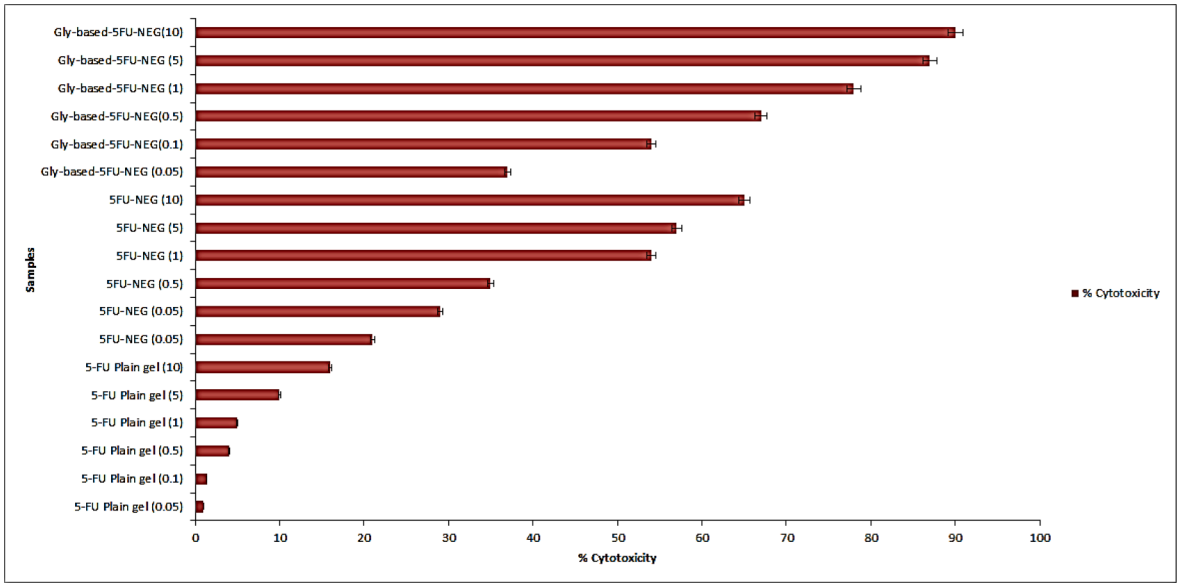


**Fig. 9.** Cytotoxicity profile of pure 5FU gel and developed test formulations of different serial dilutions in B16F10 cell lines.

**Table 7**
Evaluation of cellular uptake different test samples by MTT assay.

| Samples | %age uptake |
|---|---|
| **Control** | 0 ± 0 |
| **5FU-Gel (20 µg/mL)** | 11.5 ± 0.13 |
| **5-FU NEG (1.1 µg/mL)** | 44.3 ± 0.33 |
| **GLY-5-FU NEG (0.1 µg/mL)** | 54.6 ± 1.38** |

**$p < 0.05$, compared with 5FU gel.

**Table 8**
Drug distribution in different cell cycle phase of optimized formulations.

| Treatment Groups | IC50 (µg/ml) | G Phase | Go Phase | S Phase |
|---|---|---|---|---|
| **Untreated Control** | **10 ± 0.02** | **75 ± 1.32** | **10 ± 0.04** | **5 ± 0.02** |
| **5-FU Plain gel** | **20 ± 0.33** | **60 ± 2.43** | **30 ± 2.42** | **8 ± 0.02** |
| **5-FU-NEG** | **1.1 ± 0.09** | **30 ± 2.14** | **20 ± 1.44** | **10 ± 1.23** |
| **GLY based 5-FU-NEG** | **0.1 ± 0.001**** | **20 ± 1.55**** | **30 ± 2.88**** | **30 ± 2.43**** |

**$p < 0.05$, compared with 5-FU gel.

less prone to coalescence and phase separation, which was corroborated by the negligible coalescence observed in our samples (Liu et al., 2017). This stability is fundamental for ensuring the consistent delivery of the drug over time. Furthermore, the absence of drug precipitation within the globules is a significant finding. This indicates that the drug is well-incorporated within the NE, either solubilized in the oil phase or adequately dispersed throughout the system. The efficient encapsulation and distribution of the drug within these nano-sized carriers are critical for enhancing bioavailability, particularly for topical applications (Zhan et al., 2021).

The evaluation of a Glycyrrhizin (GLY)-based nanoemulgel (NEG) involves a comprehensive set of tests aimed at assessing various aspects of the formulation's properties, drug release, and skin permeation capabilities (Lopes et al., 2022). Each test provides valuable insights into the behavior of the nanoemulgel and its potential for pharmaceutical and topical applications for skin cancer Texture analysis remains a vital test to evaluate the sensory attributes and consistency of the NEG (Li et al., 2015). Parameters like hardness, cohesiveness, and spreadability give insights into the formulation's ease of application and user experience. Favorable texture analysis with optimum deformity and hardness results indicate that the GLY-5FU-NEG possesses a desirable texture, making it pleasant to use and promoting patient compliance (Li et al., 2015). For rheological determination, the results indicated that the GLY-5FU NEG gel exhibited a stable viscosity profile, consistent with the desired characteristics for effective topical application. The rheological properties demonstrated the gel's potential for enhanced skin permeability and retention, crucial for the therapeutic efficacy of 5-FU in melanoma treatment (Chou et al., 2018). These findings underscore the suitability of the GLY-5FU NEG formulation in maintaining a balance between spreadability and stability, key factors in the effectiveness of topical drug delivery systems. DSC analysis is still employed to study the thermal behavior of the formulation components, including the active ingredient and excipients. This test helps identify any potential interactions, phase transitions, or changes in the formulation due to temperature variations (Campos et al., 2016). Favorable DSC results can demonstrate the compatibility of the components, ensuring that the nanoemulgel remains stable and retains its properties over a range of temperatures (Campos et al., 2016). *In vitro* drug release studies are crucial to understanding the release profile of the active ingredient from the plain gel (5-FU-NEG) and Gly based 5FU-NEG (Pinho et al., 2019). By simulating physiological conditions, these tests provide insights into the formulation's release kinetics, which is crucial for controlling drug delivery rates (Kanugo, 2022). The observed burst release phenomenon in the optimized GLY-based 5-FU NEG formulation can be attributed to the eroding outer layer of 5-FU within the gel matrix. This initial burst release is advantageous for achieving rapid therapeutic effects, particularly in the treatment of superficial skin conditions such as melanoma. Subsequently, the sustained release pattern observed in the optimized GLY-based 5-FU NEG formulation can be attributed to the diffusion of the drug from the gel matrix, facilitated by the unique properties of the NE system (Pardini and Jordan, 1984). Furthermore, the release data of the optimized GLY-based 5-FU NEG formulation were fitted to various kinetics models, the highest coefficient of determination ($R^2$) was obtained for the first-order release model ($R^2 = 0.974$) (Forouz, 2020). This indicates that the release of 5-FU from the optimized GLY-based 5-FU NEG formulation follows a first-order kinetic process, suggesting that the rate of drug release is proportional to the remaining drug concentration within the gel matrix. This provides insights into the release mechanism, indicating that the drug release is governed by both diffusion and erosion processes (Fitton and Goa, 1991). *Ex-vivo* skin permeation studies involve the assessment of drug penetration through a skin membrane. This test is vital for evaluating the formulation's ability to

facilitate drug absorption into the skin layers (Kaplan et al., 2019). From the observations gathered from ex vivo permeation study, it was clearly shown that GLY-based 5-FU NEG observed superior permeability characteristics which might be attributed to its small droplet size, excellent penetration and high stability characteristics in the biological system. GLY, a natural triterpene glycoside derived from licorice root (Glycyrrhiza glabra), has gained attention for its potential as a penetration enhancer in pharmaceutical and cosmetic applications (Nokhodchi et al., 2002; Beiu et al., 2020; Kaplan et al., 2019). This enhancement mechanism can be attributed to its amphiphilic nature, enabling interactions with the skin's lipid bilayer. By perturbing this lipid structure, glycyrrhizin disrupts the barrier function of the stratum corneum, the outermost layer of the skin, consequently promoting the permeation of active compounds (Beiu et al., 2020; Kaplan et al., 2019). Moreover, glycyrrhizin's interactions with skin proteins, including keratin, can modify protein conformation and loosen the tight junctions between skin cells, thereby facilitating the movement of molecules across skin layers (Hasan et al., 2023). Additionally, its anti-inflammatory properties help maintain skin integrity by reducing inflammation-induced changes that may impede permeation. The glycyrrhizin-induced hydration of the stratum corneum softens the skin, enhancing its susceptibility to compound penetration. Furthermore, glycyrrhizin's potential to modulate tight junctions may impact their formation by influencing protein expression, potentially further increasing skin permeability (Nagaraja et al., 2021).

An in vitro cell line study in B16 F10 cells involves a series of tests aimed at understanding the impact of a compound or formulation on cultured cells. Cytotoxicity assessment is a fundamental step to determine the potential toxic effects of the glycyrrhizin-based nanoemulgel on the cultured cells. This test helps identify the concentration range at which the formulation may adversely affect cell viability (Calienni et al., 2019). By exposing the cells to different concentrations of the nanoemulgel, researchers can observe whether the formulation causes cell death, growth inhibition, or other cytotoxic effects. The possible reason behind the higher cytotoxicity of GLY-5FU-NEG formulation in comparison to 5-FU NEG is the incorporation of compatible excipient i.e. plant based natural terpene derivative GLY which promote penetration of 5-FU into cells and have additional anti-melanoma property results in synergistic anti-cancer activity and possible reduction in concentration of 5-FU for therapeutic action (Bharadwaj et al., 2019). An intracellular uptake study aims to assess how efficiently the glycyrrhizin-based nanoemulgel is internalized by the cells (Das et al., 2013). This test provides insights into the formulation's ability to penetrate cell membranes and deliver its active components intracellularly. By using technique like flow cytometry, we visualize and quantify the extent of cellular uptake (Lin et al., 2020). Favorable results would suggest that the GLY-5FU-NEG effectively enters the cells, indicating its potential for delivering therapeutic agents to the target site within the cells. This may be due to improved penetration and selective targeting of GLY into the melanoma trypsinized cells (Kurangi et al., 2021). GLY can promote the internalization of 5-FU containing nanoemulsions into the cells, allowing for improved delivery which facilitated its improved cellular uptake. Moreover, GLY has been reported to assist in the escape of nanocarrier from endosomes (Ruan et al., 2021). It can disrupt the endosomal membrane and promote the release of the encapsulated 5-FU into the cytoplasm of B16F10 cells, enhancing the intracellular uptake (Ruan et al., 2021). To evaluate the DNA content of the cells and map out the distribution of cells at various stages of the cell cycle, flow cytometry analysis was carried out. Cell cycle analysis examines the distribution of cells within different phases of the cell cycle (G1, S, G2, and M). This test helps researchers understand how the GLY-5FU-NEG affects cell division and proliferation. By using flow cytometry, researchers can identify any changes in the cell cycle profile induced by the formulation. Findings revealed significant alterations in the cell cycle profile, implying potential impacts of the developed formulations on cell cycle progression in B16F10 melanoma cells. Specifically, the observed changes in the distribution of the B16F10 melanoma cells' cell cycle indicated that the GLY-5FU-NEG formulation might possess the capability to influence cell cycle progression. The decrease in the percentage of cells in the G0/G1 phase suggests a potential disruption of cell cycle arrest, while the increase in the proportion of cells in the S and G2/M phases implies enhanced cell cycle progression or delayed cell cycle transition in the optimized formulation, compared to the 5-FU-NE gel [60]. Further investigation is warranted to elucidate the underlying molecular mechanisms involved in these effects and to evaluate the impact on cell proliferation and apoptosis.

## 5. Conclusion

The present study successfully optimized and evaluated a glycyrrhizin-based nanoemulgel for the topical delivery of 5-FU. The formulation exhibited desirable physicochemical properties, including a small particle size, appropriate zeta potential, and high drug entrapment efficiency. The in vitro release studies demonstrated sustained release of 5-FU from the nanoemulgel over a 24-hour period, indicating its potential for extended drug delivery. The cell line study using B16F10 confirmed the efficacy of the optimized nanoemulgel in delivering 5-FU to the target cells. The nanoemulgel formulation significantly reduced cell viability, indicating its potential as an effective treatment for skin conditions where 5-FU is indicated. The use of glycyrrhizin as a natural penetration enhancer in the nanoemulgel formulation offers the advantage of utilizing a safe and readily available compound. The incorporation of glycyrrhizin in the nanoemulgel system could potentially enhance the permeation of 5-FU through the skin and improve its therapeutic efficacy.

**Funding information**

The authors extend their appreciation to the Deputyship for Research and Innovation, "Ministry of Education" in Saudi Arabia for funding this research having Project Number (IFKSUOR3-618-3).

## CRediT authorship contribution statement

Conceptualization: DS, NG Funding acquisition: NAA, ABA, Data curatin: DS, NG, GDG, Writing – original draft: NG Writing – review & editing: NG and DS Visualization: DS Investigation: DS and KA Validation: KA Formal analysis: KA Methodology: DS Supervision: DS Resources: DS Project administration and Software: GDG, DS and KA.

## Declaration of competing interest

The authors declare that they have no known competing financial interests or personal relationships that could have appeared to influence the work reported in this paper.

## Acknowledgements

The authors extend their appreciation to the Deputyship for Research and Innovation, "Ministry of Education" in Saudi Arabia for funding this research having Project Number (IFKSUOR3-618-3). The authors are also thankful to ISFCP for sophisticated facilities for supporting this research work.

## References

Al-Nima, A. M., Qasim, Z. S., Al-Kotaji, M., 2020. Formulation, evaluation and antimicrobial potential of topical Licorice root extract gel. Iraqi J. Pharm., 17(1), 37-56.

Arasi, M.B., Pedini, F., Valentini, S., Felli, N., Felicetti, F., 2020. Advances in natural or synthetic nanoparticles for metastatic melanoma therapy and diagnosis. Cancers 12. https://doi.org/10.3390/cancers12102893.

Ayub, A.C., Gomes, A.D., Lima, M.V., Vianna-Soares, C.D., Ferreira, L.A., 2007. Topical delivery of fluconazole: in vitro skin penetration and permeation using emulsions as dosage forms. Drug Dev. Ind. Pharm. 33 (3), 273–280. https://doi.org/10.1080/03639040601036357.

Beiu, C., Giurcaneanu, C., Grumezescu, A., Holban, A., Popa, L., Mihai, M., 2020. Nanosystems for improved targeted therapies in melanoma. J. Clin. Med. 9 https://doi.org/10.3390/jcm9020318.

Bharadwaj, R., Haloi, J., Medhi, S., 2019. Topical delivery of methanolic root extract of Annona reticulata against skin cancer. S. Afr. J. Bot. https://doi.org/10.1016/J.SAJB.2019.06.006.

Calienni, M.N., Febres-Molina, C., Llovera, R.E., Zevallos-Delgado, C., Tuttolomondo, M. E., Paolino, D., Fresta, M., Barazorda-Ccahuana, H.L., Gómez, B., del Valle Alonso, S., Montanari, J., 2019. Nanoformulation for potential topical delivery of vismodegib in skin cancer treatment. Int. J. Pharm. 565, 108–122. https://doi.org/10.1016/j.ijpharm.2019.05.039.

Campos, P.M., Bentley, M., Torchilin, V., 2016. Nanopreparations for Skin Cancer Therapy. https://doi.org/10.1016/B978-0-323-42863-7.00001-3.

Chen, J., Zhang, X.D., 2016. Nanodelivery of Anticancer Agents in Melanoma. https://doi.org/10.1016/B978-0-12-802926-8.00015-X.

Chen, J., Shao, R., Zhang, X.D., Chen, C., 2013. Applications of nanotechnology for melanoma treatment, diagnosis, and theranostics. Int. J. Nanomed. 8, 2677–2688. https://doi.org/10.2147/IJN.S45429.

Chou, Y.P., Lin, Y.K., Chen, C.H., Fang, J.Y., 2018. Recent advances in polymeric nanosystems for treating cutaneous melanoma and its metastasis. Curr. Pharm. Des. 23 (35), 5301–5314. https://doi.org/10.2174/1381612823666170710121348.

Das, S., Das, J., Samadder, A., Paul, A., Khuda-Bukhsh, A.R., 2013. Strategic formulation of apigenin-loaded PLGA nanoparticles for intracellular trafficking, DNA targeting and improved therapeutic effects in skin melanoma in vitro. Toxicol. Lett. 223 (2), 124–138. https://doi.org/10.1016/j.toxlet.2013.08.018.

de Moura, L.D., Ribeiro, L.N.M., de Carvalho, F.V., da Silva, G.H., Fernandes, P.C.L., Brunetto, S.Q., Ramos, C.D., Velloso, L., de Araújo, D.D., de Paula, E., 2021. Docetaxel and lidocaine co-loaded (NLC-in-hydrogel) hybrid system designed for the treatment of melanoma. Pharmaceutics 13. https://doi.org/10.3390/pharmaceutics13101552.

Farhana, A., 2023. Enhancing skin cancer immunotheranostics and precision medicine through functionalized nanomodulators and nanosensors: recent development and prospects. Int. J. Mol. Sci. 24 https://doi.org/10.3390/ijms24043493.

Fitton, A., Goa, K., 1991. Azelaic acid. Drugs 41, 780–798. https://doi.org/10.2165/00003495-199141050-00007.

Forouz, F., 2020. Enhanced Topical Drug Delivery for Treatment of Human Melanoma. https://doi.org/10.14264/0cacb8a.

Hartmann, T., Perron, R., Razavi, M., 2022. Utilization of Nanoparticles, Nanodevices, and Nanotechnology in the Treatment Course of Cutaneous Melanoma. Adv. Ther., 5. DOI: 10.1002/adtp.202100208.

Hasan, N., Imran, M., Nadeem, M., Jain, D., Haider, K., Rizvi, M.M.A., Sheikh, A., Kesharwani, P., Ahmad, F.J., 2023. Formulation and development of novel lipid-based combinatorial advanced nanoformulation for effective treatment of non-melanoma skin cancer. Int. J. Pharm. 632, 122580 https://doi.org/10.1016/j.ijpharm.2023.122580.

Kanugo, A., 2022. Recent advances of nanotechnology in the treatment of skin cancer. Curr. Pharm. Biotechnol. https://doi.org/10.2174/1389201023666220404113242.

Kaplan, A., Çetin, M., Orgul, D., Taghizadehghalehjoughi, A., Hacimuftuoglu, A., Hekimoglu, S., 2019. Formulation and in vitro evaluation of topical nanoemulsion and nanoemulsion-based gels containing daidzein. J. Drug Deliv. Sci. Technol. https://doi.org/10.1016/J.JDDST.2019.04.027.

Kurangi, B., Jalalpure, S., Jagwani, S., 2021. Formulation and evaluation of resveratrol loaded cubosomal nanoformulation for topical delivery. Curr. Drug Deliv. 18 (5), 607–619. https://doi.org/10.2174/1567201817666200902150646.

Li, J., Wang, Y., Liang, R., An, X., Wang, K., Shen, G., Tu, Y., Zhu, J., Tao, J., 2015. Recent advances in targeted nanoparticles drug delivery to melanoma. Nanomedicine 11 (3), 769–794. https://doi.org/10.1016/j.nano.2014.11.006.

Lin, H., Lin, L., Choi, Y.H., Michniak-Kohn, B., 2020. Development and in-vitro evaluation of co-loaded berberine chloride and evodiamine ethosomes for treatment of melanoma. Int. J. Pharm. https://doi.org/10.1016/j.ijpharm.2020.119278.

Liu, Q., Das, M., Liu, Y., Huang, L., 2017. Targeted drug delivery to melanoma. Adv. Drug Deliv. Rev. 127, 208–221. https://doi.org/10.1016/j.addr.2017.09.016.

Lopes, J., Rodrigues, C., Gaspar, M.M., Reis, C., 2022. How to treat melanoma? the current status of innovative nanotechnological strategies and the role of minimally invasive approaches like PTT and PDT. Pharmaceutics 14. https://doi.org/10.3390/pharmaceutics14091817.

Madamsetty, V., Paul, M., Mukherjee, A., & Mukherjee, S., 2020. Functionalization of Nanomaterials and Their Application in Melanoma Cancer Theranostics. ACS Biomater. Sci. Eng., 6(1), 167-181. DOI: 10.1021/acsbiomaterials.9b01426.

Madni, A., Rahim, M.A., Mahmood, M.A., Jabar, A., Rehman, M., Shah, H., Khan, A., Tahir, N., Shah, A., 2018. Enhancement of dissolution and skin permeability of pentazocine by proniosomes and niosomal gel. AAPS PharmSciTech 19, 1544–1553. https://doi.org/10.1208/s12249-018-0985-1.

Monge-Fuentes, V., Muehlmann, L.A., de Azevedo, R.D., 2014. Perspectives on the application of nanotechnology in photodynamic therapy for the treatment of melanoma. Nano Rev. 5 https://doi.org/10.3402/nano.v5.24381.

Nagaraja, S., Basavarajappa, G.M., Attimarad, M., Pund, S., 2021. Topical nanoemulgel for the treatment of skin cancer: proof-of-technology. Pharmaceutics 13. https://doi.org/10.3390/pharmaceutics13060902.

Naves, L., Dhand, C., Venugopal, J., Rajamani, L., Ramakrishna, S., Almeida, L., 2017. Nanotechnology for the treatment of melanoma skin cancer. Prog. Biomater. 6, 13–26. https://doi.org/10.1007/s40204-017-0064-z.

Nazir, S., Khan, M.U.A., Al-Arjan, W.S., Abd Razak, S.I., Javed, A., Kadir, M.R.A., 2021. Nanocomposite hydrogels for melanoma skin cancer care and treatment: in-vitro drug delivery, drug release kinetics and anti-cancer activities. Arab. J. Chem. https://doi.org/10.1016/J.ARABJC.2021.103120.

Nicoli, S., Padula, C., Aversa, V., Vietti, B., Wertz, P.W., Millet, A., Falson, F., Govoni, P., Santi, P., 2008. Characterization of rabbit ear skin as a skin model for in vitro transdermal permeation experiments: histology, lipid composition and permeability. Skin Pharmacol. Physiol. 21 (4), 218–226. https://doi.org/10.1159/000131087.

Nokhodchi, A., Nazemiyeh, H., Ghafourian, T., Hassan-Zadeh, D., Valizadeh, H., Bahary, L.A., 2002. The effect of glycyrrhizin on the release rate and skin penetration of diclofenac sodium from topical formulations. Il Farmaco 57 (11), 883–888. https://doi.org/10.1016/S0014-827X(02)01273-6.

Pardini, R., Jordan, R.T., 1984. Anti-neoplastic activity of C205: a new topical anti-cancer formulation. Cancer Lett. 23 (3), 273–277. https://doi.org/10.1016/0304-3835(84)90094-6.

Pinho, J.O., Matias, M., Gaspar, M.M., 2019. Emergent nanotechnological strategies for systemic chemotherapy against melanoma. Nanomaterials 9. https://doi.org/10.3390/nano9101455.

Pund, S., Pawar, S., Gangurde, S., Divate, D., 2015. Transcutaneous delivery of leflunomide nanoemulgel: mechanistic investigation into physicomechanical characteristics, in vitro anti-psoriatic and anti-melanoma activity. Int. J. Pharm. 487 (1–2), 148–156. https://doi.org/10.1016/j.ijpharm.2015.04.015.

Quan, W., Kong, S., Ouyang, Q., Tao, J., Lu, S., Huang, Y., Li, S., Luo, H., 2021. Use of 18β-glycyrrhetinic acid nanocrystals to enhance anti-inflammatory activity by improving topical delivery. Colloids Surf. B Biointerfaces 205, 111791. https://doi.org/10.1016/j.colsurfb.2021.111791.

Raju, D., Shanmugan, S., Bennet, M., 2017. On Feature Image Recognition of Melanoma Using Nanotechnology Applications. https://doi.org/10.2412/MMSE.82.25.192.

Rigon, R., Oyafuso, M.H., Fujimura, A.T., Gonçalez, M., do Prado, A. H., Gremião, M., & Chorilli, M., 2015. Nanotechnology-based drug delivery Systems for Melanoma Antitumoral Therapy: a review. BioMed Res. Int. 2015 https://doi.org/10.1155/2015/841817.

Ruan, L., Song, G., Zhang, X., Liu, T., Sun, Y., Zhu, J., Zeng, Z., Jiang, G., 2021. Transdermal delivery of multifunctional CaO2@Mn-PDA nanoformulations by microneedles for NIR-induced synergistic therapy against skin melanoma. Biomaterials Sci. 9 (20), 6830–6841. https://doi.org/10.1039/D1BM01117K.

Running, L.S., Espinal, R., Hepel, M., 2018. Controlled release of targeted chemotherapeutic drug dabrafenib for melanoma cancers monitored using surface-enhanced raman scattering (SERS) spectroscopy. Mediterr. J. Chem. 7, 18–27. https://doi.org/10.13171/MJC71/01803171500-HEPEL.

Sack, M., Alili, L., Karaman, E., Das, S., Gupta, A., Seal, S., Brenneisen, P., 2014. Combination of conventional chemotherapeutics with redox-active cerium oxide nanoparticles—A novel aspect in cancer therapy. Mol. Cancer Ther. 13, 1740–1749. https://doi.org/10.1158/1535-7163.MCT-13-0950.

Sapra, B., Jain, S., Tiwary, A.K., 2008. Transdermal delivery of carvedilol containing glycyrrhizin and chitosan as permeation enhancers: biochemical, biophysical, microscopic and pharmacodynamic evaluation. Drug Deliv. 15 (7), 443–454. https://doi.org/10.1080/10717540802241628.

Simon, A., Amaro, M.I., Healy, A.M., Cabral, L.M., de Sousa, V.P., 2016. Comparative evaluation of rivastigmine permeation from a transdermal system in the Franz cell using synthetic membranes and pig ear skin with in vivo-in vitro correlation. Int. J. Pharm. 512 (1), 234–241. https://doi.org/10.1016/j.ijpharm.2016.05.053.

Tang, J., Hou, X., Yang, C., Li, Y., Xin, Y., Guo, W., Wei, Z., Liu, Y.Q., Jiang, G., 2017. Recent developments in nanomedicine for melanoma treatment. Int. J. Cancer. https://doi.org/10.1002/ijc.30708.

Wang, Y., Chang, T., 2021. A polymer–lipid membrane artificial cell nanocarrier containing enzyme–oxygen biotherapeutic inhibits the growth of B16F10 melanoma in 3D culture and in a mouse model. Artif. Cells Nanomed. Biotechnol. 49, 461–470. https://doi.org/10.1080/21691401.2021.1918134.

Wu, Z., Zhuang, H., Ma, B., Xiao, Y., Koç, B., Zhu, Y., Wu, C., 2021. Manganese-doped calcium silicate nanowire composite hydrogels for melanoma treatment and wound healing. Research 2021. https://doi.org/10.34133/2021/9780943.

Zhan, X., Teng, W., Sun, K., He, J., Yang, J., Tian, J., Huang, X., Zhou, L., Zhou, C., 2021. CD47-mediated DTIC-loaded chitosan oligosaccharide-grafted nGO for synergistic chemo-photothermal therapy against malignant melanoma. Mater. Sci. Eng. C Mater. Biol. Appl. 123, 112014 https://doi.org/10.1016/j.msec.2021.112014.

Zhao, Y., Zhou, Y., Yang, D., Gao, X., Wen, T., Fu, J., Wen, X., Quan, G., Pan, X., Wu, C., 2021. Intelligent and spatiotemporal drug release based on multifunctional nanoparticle-integrated dissolving microneedle system for synergetic chemo-photothermal therapy to eradicate melanoma. Acta Biomater. https://doi.org/10.1016/j.actbio.2021.09.009.